



Published in final edited form as:

Cancer Res. 2011 November 15; 71(22): 7103–7112. doi:10.1158/0008-5472.CAN-10-3192.

Decreased Lymphangiogenesis and Lymph Node Metastasis by mTOR Inhibition in Head and Neck Cancer

Vyomesh Patel¹, Christina A. Marsh¹, Robert T. Dorsam^{1,4}, Constantinos M. Mikelis¹, Andrius Masedunskas¹, Panomwat Amornphimoltham¹, Cherie Ann Nathan², Bhuvanesh Singh³, Roberto Weigert¹, Alfredo A. Molinolo¹, and J. Silvio Gutkind^{1,*}

¹Oral and Pharyngeal Cancer Branch, National Institute of Dental Research, National Institutes of Health, Bethesda, MD

²Department of Otolaryngology - Head and Neck Surgery, Louisiana State University Health Sciences Center, Shreveport, LA

³Laboratory of Epithelial Cancer Biology, Head and Neck Service, Memorial Sloan-Kettering Cancer Center, New York, NY

Abstract

Despite our improved understanding of cancer, the 5-year survival rate for head and neck squamous cell carcinomas (HNSCC) patients remains relatively unchanged at 50% for the past three decades. HNSCC often metastasize to locoregional lymph nodes, and lymph node involvement represents one of the most important prognostic factors of poor clinical outcome. Among the multiple dysregulated molecular mechanism in HNSCC, emerging basic, preclinical, and clinical findings support the importance of the mTOR signaling route in HNSCC progression. Indeed, we observed here that the activation of mTOR is a widespread event in clinical specimens of HNSCC invading locoregional lymph nodes. We developed an orthotopic model of HNSCC consisting in the implantation of HNSCC cells into the tongues of immunocompromised mice. These orthotopic tumors spontaneously metastasize to the cervical lymph nodes, where the presence of HNSCC cells can be revealed by histological and immunohistochemical evaluation. Both primary and metastatic experimental HNSCC lesions exhibited elevated mTOR activity. The ability to monitor and quantitate lymph node invasion in this model system enabled us to explore whether the blockade of mTOR could impact on HNSCC metastasis. We found that inhibition of mTOR with rapamycin and the rapalog RAD001 diminished lymphangiogenesis in the primary tumors and prevented the dissemination of HNSCC cancer cells to the cervical lymph nodes, thereby prolonging animal survival. These findings may provide a rationale for the future clinical evaluation of mTOR inhibitors, including rapamycin and its analogs, as part of a molecular-targeted metastasis preventive strategy for the treatment of HNSCC patients.

Keywords

mTOR; metastasis; oral cancer; targeted therapies; signal transduction

*Corresponding Author: Oral and Pharyngeal Cancer Branch, National Institute of Dental and Craniofacial Research, NIH, 30 Convent Drive, Building 30, Room 211, Bethesda, MD 20892-4330. Phone: (301) 496-6259; Fax: (301) 402-0823; sg39v@nih.gov.

⁴Current Address, Food and Drug Administration, Silver Spring, MD.

Disclosure of Potential Conflicts of Interest: The authors indicate no disclosures of potential conflicts of interest.

Introduction

With approximately 500,000 new cases per year worldwide (1) and more than 11,000 expected deaths in 2009 in the US alone (2), squamous cell carcinoma of the head and neck (HNSCC) ranks sixth among the most common cancers in the world (3). Despite clear advancements in our understanding of cancer as a disease, the 5-year survival rate for HNSCC remains relatively unchanged at 50% for the past 3 decades (2, 3). Several important factors contribute to this bleak scenario, including late presentation and consequent delay in the diagnosis of HNSCC lesions, concomitant with the limited availability of effective therapeutic options to reduce the morbidity and mortality of advanced HNSCC cases (4–7). In this regard, the head and neck region includes a large fraction of all the lymph nodes of the human body, and with this rich lymphatic system, HNSCC has a high propensity to metastasize to locoregional lymph nodes (5, 8–12). Even in patients with no clinical evidence of lymph nodal metastasis (N0), the incidence of occult metastasis ranges from 10 to 50% (8–11), and the status of cervical lymph node metastasis is often considered the single most important prognostic factor in HNSCC, with the presence of lymph node involvement decreasing the overall survival by nearly 50% (5, 9, 12).

Of interest, among the multiple molecular mechanism dysregulated in HNSCC, emerging basic, preclinical, and clinical findings support the importance of Akt/mTOR signaling route in HNSCC progression (reviewed in (7)). Indeed, activation of mTOR and Akt, the latter acting upstream from mTOR, has been observed in more than 80% of all HNSCC lesions (6) often correlating with poor prognosis (13, 14). The activation of mTOR can result from the enhanced expression and activity of epidermal growth factor receptors (EGFRs) that characterize HNSCC (15), as well as by the overexpression or the presence of activating mutations in the catalytic subunit of PI3K α (16) or the decreased expression of the PIP₃ phosphatase PTEN (17). Furthermore, interfering with mTOR activity in its complex 1 (mTORC1) by the use of specific inhibitors, such as rapamycin (sirolimus) and its analogs (e.g., CCI-779, also known as temsirolimus, and RAD001, known as everolimus), has been shown to provoke the rapid regression of HNSCC tumor xenografts (18), to prevent tumor re-growth in a minimal residual HNSCC xenograft model (19), and to decrease tumor burden and the malignant conversion of potential HNSCC precancerous lesions in multiple genetically-defined and chemically-induced animal models of HNSCC (20–22). These observations prompted us to examine whether mTOR is activated in human HNSCC lymph nodes metastasis, and whether blocking mTOR prevents the metastatic spread of primary HNSCC lesions. We show here that the activation of mTOR is a widespread event in clinical specimens of HNSCC invading locoregional lymph nodes. Furthermore, the prolonged treatment with rapamycin and RAD001 diminished the dissemination of HNSCC cancer cells to the cervical lymph nodes in a newly developed orthotopic HNSCC model, thereby prolonging animal survival. Thus, the use of mTOR inhibitors may represent a novel molecular-targeted approach for metastasis prevention in HNSCC patients.

Materials and Methods

Chemical and Reagents and Cell Culture

All chemicals and reagents were from Sigma-Aldrich (St Louis, MO, USA), unless indicated. UMSCC2 and UMSCC17B cells were cultured as previously described (23, 24) in DMEM supplemented with 10% fetal bovine serum (FBS), at 37°C in 95% air/5% CO₂, and both cell lines underwent DNA authentication (Genetica DNA Laboratories, Inc.) prior to the described experiments to ensure consistency in cell identity.

Establishment and Treatment of Orthotopic Tumor Xenografts in SCID-NOD Mice

All animal studies were carried out according to NIH-approved protocols (ASP# 10–569), in compliance with the NIH Guide for the Care and Use of Laboratory Animals. Female SCID-NOD mice (NCI, Frederick, MD, USA), 4–6 weeks of age and weighing 18–20 g were used in the study were housed in appropriate sterile filter-capped cages and fed and watered *ad libitum*. All cell and animal handling and tumor transplantation into the tongue are described in detail in Supplemental Material. Briefly, all animals bearing orthotopic HNSCC tumors underwent weekly evaluation of the tongue for disease onset, and the observed lesions were assessed for length and width and tumor volume was determined as described previously (18). Animals were euthanized at the indicated time points and the cervical lymph nodes assessed for evidence of metastases.

Histopathological and Immunohistological Analysis

For histopathology, after fixing each tongue was cut into four sections of approximately the same thickness, following its major axis (20), and tissue processing, immunohistochemical analysis, image acquisition, and staining quantification were performed as described in Supplemental Material. Masson trichrome staining was performed on formalin-fixed, paraffin embedded tissues as previously described (25).

Statistical analysis

One-way ANOVA followed by Bonferroni's or Newman-Keuls multiple comparison tests was used to analyze the differences of tumor mass volume between experimental groups and differences between immunohistochemical quantification of each group. The Mann-Whitney test was used to evaluate differences in total tumor area. Data analysis was done using GraphPad Prism version 5.00 for Windows (GraphPad Software, La Jolla, CA, USA); P values of <0.05 were considered statistically significant for each analysis as described in detail in Supplemental Material.

Results

As we have previously reported, the activation of mTOR is a widespread event in HNSCC, as judged by the immunohistochemical analysis of the presence of the phospho-serine ribosomal protein S6 (pS6) in representative human HNSCC tissue sections (Figure 1A). These tumors are highly angiogenic, as revealed by the use of the vascular endothelial marker CD31 showing blood vessels within the stroma adjacent to the tumoral mass positive for pS6 (Figure 1A). Most human HNSCC lesions are also highly lymphangiogenic (26), reflected by the presence of intratumoral lymphatic vessels staining positive for lymphatic vessel endothelial receptor 1 (LYVE-1). Indeed, the microvessel density of vascular and lymphatic vessels were comparable when analyzing consecutive tissue sections of a representative group of HNSCC lesions (n=5) (Figure 1B). Of interest, the presence of active mTOR was also clearly observed in the epithelial cells of all human invaded HNSCC lymph nodes analyzed (n=8); only isolated lymphocytic subpopulations showed cytoplasmic immunoreactivity in normal, non-invaded areas in human lymph nodes (Figure 1C). Similarly, we also observed elevated levels of the serine-473 phosphorylated form of Akt (pAkt^{S473}), a downstream target of mTOR in its complex mTORC2 (27), in most tumor cells from all invaded lymph nodes evaluated (n=8) (Figure 1C). All malignant cells displaying elevated pS6 and pAkt^{S473} in invading tumors were of epithelial origin, as revealed by staining adjacent tissue sections for human cytokeratins (Figure 1C).

To begin addressing whether molecular-targeted approaches could be used to prevent the spread of HNSCC to locoregional lymph nodes, we took advantage of the availability of highly invasive HNSCC cells to develop an orthotopic model of HNSCC metastasis. Few

metastatic models are currently available in which lymph node metastases develop, albeit with limited efficiency (28–30). In particular, the evaluation of a large panel of HNSCC-derived cells led to the identification of two highly invasive human HNSCC cell lines, UMSCC2 and UMSCC17B. When orthotopically injected into the tongue of SCID/NOD mice, these HNSCC cells grew as highly aggressive tumors, invading the muscle and all surrounding tissues. For example, intraepithelial invasion was readily visible under microscopic evaluation (Figures 2A–B for UMSCC2 cells, and Supp. Figure 1A–B for UMSCC17B). Remarkably, these HNSCC cells also invaded the nerves and local lymph nodes, with visible tumor masses growing inside the lymphatic vessels (Figures 2C, D, and Supp. Figure 1C, D). These tumors are highly lymphangiogenic, reflecting a characteristic displayed by most human HNSCC lesions (26). Intratumoral lymphatic vessels staining positive for LYVE-1 were visible within the tumoral mass (Figure 2E and Supp. Figure 1E). The adjacent muscle, which has extensive lymphatic networks, served as a positive control. These tumors are also highly angiogenic, as revealed by CD31 staining.

We next injected India ink orthotopically into lateral tongue in order to visualize the ink particles into the subcapsular area of the draining cervical lymph nodes (Figure 3A–B). This enabled us to identify lymphatic drainage to four to five readily resectable cervical lymph nodes. Indeed, the metastatic spread of HNSCC cells growing orthotopically into the tongue could be visualized in hematoxylin-eosin (H&E) stained lymph node sections as compared to non-invaded lymph nodes (Figures 3C–E and Supp. Figures 2 A–D). Nearly all mice in the initial cohorts had at least one or more invaded lymph nodes when sacrificed 40 days after tumor implantation into the tongue (Figure 3F and Supp. Figure 2E). This provided a simple and quantitative approach to examine the yet to be identified factors contributing to lymph node metastasis, and to attempt to halt this life threatening process. Non-invaded lymph preserved their rich cortical network of normal lymphatic vessels (Figure 3G and Supp. Figure 2F), whereas in metastatic lymph nodes, the tumor mass often displaces the lymphatic ducts (Figure 3H and Supp. Figure 2G).

In normal murine oral mucosa and skin, mTOR is activated in the suprabasal layers lacking proliferative capacity, as judged by the accumulation pS6 (Figure 4A and Supp. Figure 3A). In contrast, the tumor area displayed high levels of pS6 throughout (Figure 4A and Supp. Figure 3A). Similarly, the invaded lymph nodes displayed high levels of pS6, however the staining was not homogenous, with necrotic areas and their adjacent cells likely harboring lower mTOR activity (Figure 4B and Supp. Figure 3B). Thus, both experimental and human HNSCC metastatic lesions are characterized by the presence of active mTOR pathway. Rapamycin and RAD001, which block mTOR in its complex mTORC1 (27), abolished the detection of pS6 positive cells in the primary tumor site and invaded lymph nodes after its administration to orthotopic tumor bearing mice (Figures 4C–D and Supp. Figure 3C–D), confirming that the accumulation of pS6 reflects the aberrant activity of mTOR in these tumoral lesions. Interestingly, rapamycin and RAD001 also reduced pAkt^{S473} levels in the primary tongue lesions and their metastases, suggesting that these rapalogs can also reduce mTORC2 activity in HNSCC, likely indirectly, as observed after prolonged treatment with rapamycin of cultured cells (31).

These observations prompted us to explore the consequences of treating mice harboring HNSCC tumors with rapamycin and RAD001. Treatment was initiated approximately 10 days after tumor implantation into the tongue when primary tumors were visible in all mice. As shown in Figures 5A–D and Supp. Figures 4A–D, the impact of rapamycin treatment was remarkable. Weekly tongue evaluation revealed a significant tumor growth inhibition caused by rapamycin and RAD001 administration (Figure 5A and Supp. Figure 4A). Typical examples of tumor-bearing mice treated with vehicle control, rapamycin, and RAD001 for approximately 2–3 weeks are depicted (Figure 5B and Supp. Figure 4B). The orthotopic

tongue HNSCC model enabled the readily visualization of the tumoral lesions in the representative control and treated groups (Figure 5C and Supp. Figure 4C). Quantification of the compromised tumoral area in each tongue showed a highly significant reduction of the affected tongue surface (Figure 5D and Supp. Figure 4D).

The residual tumor in rapamycin and RAD001 treated mice at the end of the observation period showed areas of squamous differentiation and fibrosis, in contrast to control treated mice that showed active areas of cell growth (Figures 6A-D and Supp. Figure 5A-D). Of interest, rapamycin and RAD001 did not affect the vascular microvessel density of the tumoral lesions and normal tissues in this orthotopic model (Figure 6E and Supp. Figure 5E). However, they had a dramatic effect on the lymphatic system, as it prevented intratumoral lymphangiogenesis without perturbing the normal distribution of lymphatic vessels in the oral mucosa and muscle (Figure 6E and Supp. Figure 5E). Aligned with this observation, rapamycin inhibits potently the proliferation of human lymphatic endothelial cells (Supp. Figure 6). On the other hand, the ability to monitor and quantitate lymph node invasion in this model system enabled us to explore whether the blockade of mTOR with rapamycin could impact on HNSCC metastasis. As shown in Figure 6F and Supp. Figure 5F, rapamycin and RAD001 treatment caused a remarkable decrease in the number of invaded lymph nodes, which was reflected in a significant increase in the overall survival of all rapamycin and RAD001 treated animals (Figure 6G and Supp. Figure 5G).

Discussion

Newly gained molecular understanding of HNSCC initiation and tumor evolution may soon afford the opportunity to delay or halt tumor progression. In this regard, among the multiple aberrant genetic, epigenetic, and signaling events known to occur in HNSCC, the persistent activation of the Akt/mTOR pathway has emerged as potential drug target for HNSCC treatment. As supported by extensive preclinical investigation, the use of mTOR inhibitors, including rapamycin (sirolimus) and its analogs, CCI-779 (temserolimus) and RAD001 (everolimus), can dramatically reduce tumor burden and even recurrence in HNSCC tumor xenografts and in chemically-induced and genetically-defined animal models recapitulating HNSCC initiation and progression (18–22). Furthermore, recent clinical evaluation of temserolimus as neoadjuvant prior to definitive treatment has revealed that all predicted biochemical targets for mTOR inhibitors in this tumor type are hit in the clinical setting, at clinically relevant doses and with limited side effects, resulting in cancer cell apoptosis and tumor shrinkage (32). We now show that activation of the mTOR pathway is a frequent event in human metastatic HNSCC lesions. Furthermore, by the use of an orthotopic model of HNSCC in which the local tumoral invasion and lymph node metastasis can be readily assessed, we now show that mTOR inhibition with rapamycin can reduce tumoral growth in the tongue, one of its most frequent sites. As the immune system plays an important role in tumor metastasis, the implantation of human HNSCC cells in immunodeficient mice may not reflect fully the clinical situation. While keeping this potential limitation in mind, this orthotopic animal model revealed that the treatment with rapamycin prevents the metastatic spread of the HNSCC lesions, thereby prolonging animal survival.

The blockade of mTOR in experimental and clinical HNSCC lesions leads to a rapid decrease in the phosphorylated state of S6 and 4EBP1 (18, 20, 32), two downstream targets of the mTOR complex 1 (mTORC1) (27), which also serves as a biomarker for the validation of the biochemical activity of mTOR inhibitors in their target tissues. In HNSCC, rapamycin also causes a rapid decrease in the phosphorylation of Akt in serine 473 (18–20), a target for mTORC2 (27), suggesting that, as shown in cultured cell systems (31), prolonged exposure to rapamycin and its analogs can reduce mTORC2 activity, likely by an indirect, yet unknown mechanism. Similarly, we have observed a rapid blockade of

mTORC2 in the HNSCC orthotopic model system, as judged by decreased levels of pAkt^{S473}. This effect could contribute to the antimetastatic activity of rapamycin, as mTORC2 is known to be involved in polarized cell migration in multiple cell types and even in model organisms (33, 34). Thus, the blockade of mTORC2 in HNSCC might result in reduced migration of cancer cells towards chemoattractants often implicated in HNSCC metastasis, a possibility that is under current investigation.

Of interest, melanoma and HNSCC are one of the few cancers in which intratumoral lymphangiogenesis is known to occur (35). Aligned with these observations, while angiogenesis is a frequent event in HNSCC models, we noticed the formation of a remarkable network of intratumoral lymphatic vessels in the primary tumor site, which was only observed in the orthotopic HNSCC system but not when tumors were implanted in other anatomical locations. The release of multiple lymphangiogenic growth factors by HNSCC and stromal cells within the tumoral microenvironment in the tongue may account for this remarkable pro-lymphangiogenic activity of orthotopically implanted HNSCC cells and their metastatic potential (36–41), an issue that warrants further investigation. We also observed the growth of invading HNSCC cells within the lymphatic vessels, together suggesting that HNSCC cancer cells can promote the growth and recruitment of lymphatic endothelial cells or their progenitors, and support their survival within the tumor microenvironment. This was nearly completely prevented by rapamycin and RAD001 treatment, supporting an anti-lymphangiogenic function of mTOR inhibitors when administered to mice bearing tumors in their natural microenvironment. This effect likely involves the impact of these rapalogs on mTOR function in the tumor cells and/or in the lymphatic endothelial cells, hence preventing lymphangiogenic signaling. While these possibilities are under investigation, we can conclude that our findings support a unique anti-lymphangiogenic function of mTOR inhibitors, which could have multiple beneficial clinical implications. Indeed, while further work may be required to define precisely how mTOR inhibitors act in HNSCC, the emerging information suggests that rapamycin may exert its antitumoral activity at multiple steps, reducing the growth and size of the primary tumor, preventing the formation of intratumoral lymphatic vessels, and likely reducing the migratory activity of HNSCC cells towards the lymph nodes, thus preventing the locoregional metastatic spread of primary HNSCC lesions.

Among the factors influencing patient outcome, the presence of lymph node metastasis at the time of diagnosis represents the most important factor predicting a poor prognosis (5, 9–12). Unfortunately, tumor recurrence in successfully treated HNSCC patients is a frequent event, often accompanied with metastatic disease even in prior lymph node negative cases (42). Indeed, HNSCC patients often succumb to metastatic disease, compromising both quality of life and overall life expectancy. Unfortunately, there are still limited therapeutic options to prevent disease progression and locoregional and distant HNSCC spread. In this regard, the emerging preclinical and clinical information regarding the promising beneficial effects of mTOR inhibitors in HNSCC and our present findings can now be exploited to prevent HNSCC recurrence and metastasis. Specifically, we can envision that the present study and prior reports may provide a rationale for the future clinical evaluation of rapamycin and its analogs in an adjuvant setting, as part of a molecular targeted strategy for metastasis prevention after definitive treatment.

Supplementary Material

Refer to Web version on PubMed Central for supplementary material.

Acknowledgments

Financial Support: This work was supported by the Intramural Program of the National Institute of Dental and Craniofacial Research, National Institutes of Health.

Dr. Alexander Sorokin (University of Pittsburgh) and Dr. Thomas Carey (University of Michigan) for the UMSCC2 and UMSCC17B cell lines, respectively.

References

1. Parkin DM, Bray F, Ferlay J, Pisani P. Global cancer statistics, 2002. *CA Cancer J Clin.* 2005; 55:74–108. [PubMed: 15761078]
2. Jemal A, Siegel R, Ward E, Hao Y, Xu J, Thun MJ. Cancer statistics, 2009. *CA Cancer J Clin.* 2009; 59:225–49. [PubMed: 19474385]
3. Warnakulasuriya S. Global epidemiology of oral and oropharyngeal cancer. *Oral Oncol.* 2009; 45:309–16. [PubMed: 18804401]
4. Haddad RI, Shin DM. Recent advances in head and neck cancer. *N Engl J Med.* 2008; 359:1143–54. [PubMed: 18784104]
5. Forastiere A, Koch W, Trotti A, Sidransky D. Head and neck cancer. *N Engl J Med.* 2001; 345:1890–900. [PubMed: 11756581]
6. Molinolo AA, Hewitt SM, Amornphimoltham P, Keelawat S, Rangdaeng S, Meneses Garcia A, et al. Dissecting the Akt/mammalian target of rapamycin signaling network: emerging results from the head and neck cancer tissue array initiative. *Clin Cancer Res.* 2007; 13:4964–73. [PubMed: 17785546]
7. Molinolo AA, Amornphimoltham P, Squarize CH, Castilho RM, Patel V, Gutkind JS. Dysregulated molecular networks in head and neck carcinogenesis. *Oral Oncol.* 2009; 45:324–34. [PubMed: 18805044]
8. Shah JP, Candela FC, Poddar AK. The patterns of cervical lymph node metastases from squamous carcinoma of the oral cavity. *Cancer.* 1990; 66:109–13. [PubMed: 2354399]
9. Kuriakose MA, Trivedi NP. Sentinel node biopsy in head and neck squamous cell carcinoma. *Curr Opin Otolaryngol Head Neck Surg.* 2009; 17:100–10. [PubMed: 19337128]
10. Clark JR, Naranjo N, Franklin JH, de Almeida J, Gullane PJ. Established prognostic variables in N0 oral carcinoma. *Otolaryngol Head Neck Surg.* 2006; 135:748–53. [PubMed: 17071306]
11. Vokes EE, Weichselbaum RR, Lippman SM, Hong WK. Head and neck cancer. *N Engl J Med.* 1993; 328:184–94. [PubMed: 8417385]
12. Leemans CR, Tiwari R, Nauta JJ, van der Waal I, Snow GB. Recurrence at the primary site in head and neck cancer and the significance of neck lymph node metastases as a prognostic factor. *Cancer.* 1994; 73:187–90. [PubMed: 8275423]
13. Massarelli E, Liu DD, Lee JJ, El-Naggar AK, Lo Muzio L, Staibano S, et al. Akt activation correlates with adverse outcome in tongue cancer. *Cancer.* 2005; 104:2430–6. [PubMed: 16245318]
14. Yu Z, Weinberger PM, Sasaki C, Egleston BL, Speier Wf, Haffty B, et al. Phosphorylation of Akt (Ser473) predicts poor clinical outcome in oropharyngeal squamous cell cancer. *Cancer Epidemiol Biomarkers Prev.* 2007; 16:553–8. [PubMed: 17372251]
15. Kalyankrishna S, Grandis JR. Epidermal growth factor receptor biology in head and neck cancer. *J Clin Oncol.* 2006; 24:2666–72. [PubMed: 16763281]
16. Fenic I, Steger K, Gruber C, Arens C, Woenckhaus J. Analysis of PIK3CA and Akt/protein kinase B in head and neck squamous cell carcinoma. *Oncol Rep.* 2007; 18:253–9. [PubMed: 17549376]
17. Lee JJ, Soria JC, Hassan KA, El-Naggar AK, Tang X, Liu DD, et al. Loss of PTEN expression as a prognostic marker for tongue cancer. *Arch Otolaryngol Head Neck Surg.* 2001; 127:1441–5. [PubMed: 11735811]
18. Amornphimoltham P, Patel V, Sodhi A, Nikitakis NG, Sauk JJ, Sausville EA, et al. Mammalian target of rapamycin, a molecular target in squamous cell carcinomas of the head and neck. *Cancer Res.* 2005; 65:9953–61. [PubMed: 16267020]

19. Nathan CO, Amirghahari N, Rong X, Giordano T, Sibley D, Nordberg M, et al. Mammalian target of rapamycin inhibitors as possible adjuvant therapy for microscopic residual disease in head and neck squamous cell cancer. *Cancer Res.* 2007; 67:2160–8. [PubMed: 17332346]
20. Czerninski R, Amornphimoltham P, Patel V, Molinolo AA, Gutkind JS. Targeting mammalian target of rapamycin by rapamycin prevents tumor progression in an oral-specific chemical carcinogenesis model. *Cancer Prev Res (Phila Pa).* 2009; 2:27–36.
21. Raimondi AR, Molinolo A, Gutkind JS. Rapamycin prevents early onset of tumorigenesis in an oral-specific K-ras and p53 two-hit carcinogenesis model. *Cancer Res.* 2009; 69:4159–66. [PubMed: 19435901]
22. Amornphimoltham P, Leelahavanichkul K, Molinolo A, Patel V, Gutkind JS. Inhibition of Mammalian target of rapamycin by rapamycin causes the regression of carcinogen-induced skin tumor lesions. *Clin Cancer Res.* 2008; 14:8094–101. [PubMed: 19073969]
23. Zhao M, Sano D, Pickering CR, Jasser SA, Henderson YC, Clayman GL, et al. Assembly And Initial Characterization Of A Panel Of 85 Genomically Validated Cell Lines From Diverse Head And Neck Tumor Sites. *Clin Cancer Res.* 2011
24. Duex JE, Sorkin A. RNA interference screen identifies Usp18 as a regulator of epidermal growth factor receptor synthesis. *Mol Biol Cell.* 2009; 20:1833–44. [PubMed: 19158387]
25. List K, Kosa P, Szabo R, Bey AL, Wang CB, Molinolo A, et al. Epithelial integrity is maintained by a matriptase-dependent proteolytic pathway. *Am J Pathol.* 2009; 175:1453–63. [PubMed: 19717635]
26. Miyahara M, Tanuma J, Sugihara K, Semba I. Tumor lymphangiogenesis correlates with lymph node metastasis and clinicopathologic parameters in oral squamous cell carcinoma. *Cancer.* 2007; 110:1287–94. [PubMed: 17674352]
27. Guertin DA, Sabatini DM. Defining the role of mTOR in cancer. *Cancer Cell.* 2007; 12:9–22. [PubMed: 17613433]
28. Myers JN, Holsinger FC, Jasser SA, Bekele BN, Fidler IJ. An orthotopic nude mouse model of oral tongue squamous cell carcinoma. *Clin Cancer Res.* 2002; 8:293–8. [PubMed: 11801572]
29. Sano D, Myers JN. Xenograft models of head and neck cancers. *Head Neck Oncol.* 2009; 1:32. [PubMed: 19678942]
30. Kawashiri S, Kumagai S, Kojima K, Harada H, Yamamoto E. Development of a new invasion and metastasis model of human oral squamous cell carcinomas. *Eur J Cancer B Oral Oncol.* 1995; 31B:216–21. [PubMed: 7492915]
31. Sarbassov DD, Ali SM, Sengupta S, Sheen JH, Hsu PP, Bagley AF, et al. Prolonged rapamycin treatment inhibits mTORC2 assembly and Akt/PKB. *Mol Cell.* 2006; 22:159–68. [PubMed: 16603397]
32. Ekshyyan O, Mills GM, Lian T, Amirghahari N, Rong X, Lowery-Nordberg M, et al. Pharmacodynamic evaluation of temsirolimus in patients with newly diagnosed advanced-stage head and neck squamous cell carcinoma. *Head Neck.* 2010
33. Hernandez-Negrete I, Carretero-Ortega J, Rosenfeldt H, Hernandez-Garcia R, Calderon-Salinas JV, Reyes-Cruz G, et al. P-Rex1 links mammalian target of rapamycin signaling to Rac activation and cell migration. *J Biol Chem.* 2007; 282:23708–15. [PubMed: 17565979]
34. Kamimura Y, Xiong Y, Iglesias PA, Hoeller O, Bolourani P, Devreotes PN. PIP3-independent activation of TorC2 and PKB at the cell's leading edge mediates chemotaxis. *Curr Biol.* 2008; 18:1034–43. [PubMed: 18635356]
35. Pepper MS, Skobe M. Lymphatic endothelium: morphological, molecular and functional properties. *J Cell Biol.* 2003; 163:209–13. [PubMed: 14581448]
36. Cao R, Bjorndahl MA, Gallego MI, Chen S, Religa P, Hansen AJ, et al. Hepatocyte growth factor is a lymphangiogenic factor with an indirect mechanism of action. *Blood.* 2006; 107:3531–6. [PubMed: 16424394]
37. Bjorndahl M, Cao R, Nissen LJ, Clasper S, Johnson LA, Xue Y, et al. Insulin-like growth factors 1 and 2 induce lymphangiogenesis in vivo. *Proc Natl Acad Sci U S A.* 2005; 102:15593–8. [PubMed: 16230630]

38. Religa P, Cao R, Bjordahl M, Zhou Z, Zhu Z, Cao Y. Presence of bone marrow-derived circulating progenitor endothelial cells in the newly formed lymphatic vessels. *Blood*. 2005; 106:4184–90. [PubMed: 16141354]
39. Bjordahl MA, Cao R, Burton JB, Brakenhielm E, Religa P, Galter D, et al. Vascular endothelial growth factor-a promotes peritumoral lymphangiogenesis and lymphatic metastasis. *Cancer Res*. 2005; 65:9261–8. [PubMed: 16230387]
40. Cao R, Bjordahl MA, Religa P, Clasper S, Garvin S, Galter D, et al. PDGF-BB induces intratumoral lymphangiogenesis and promotes lymphatic metastasis. *Cancer Cell*. 2004; 6:333–45. [PubMed: 15488757]
41. Cao Y. Opinion: emerging mechanisms of tumour lymphangiogenesis and lymphatic metastasis. *Nat Rev Cancer*. 2005; 5:735–43. [PubMed: 16079909]
42. Coatesworth AP, Tsikoudas A, MacLennan K. The cause of death in patients with head and neck squamous cell carcinoma. *J Laryngol Otol*. 2002; 116:269–71. [PubMed: 11945186]

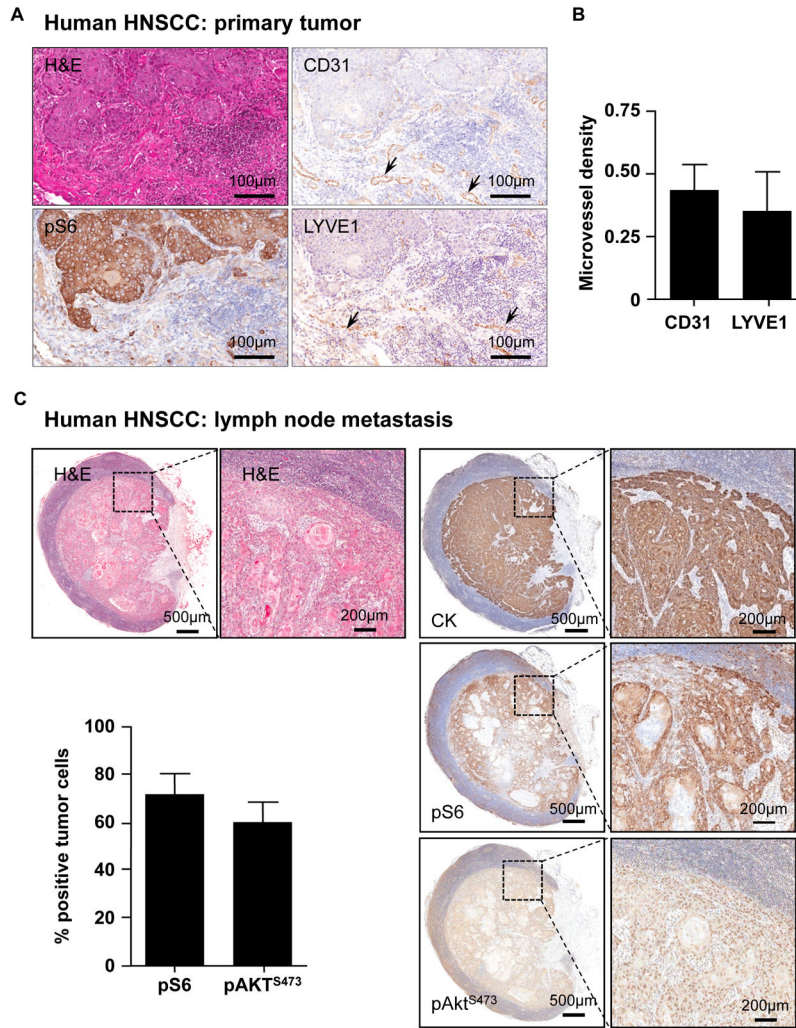


Figure 1. Activation of mTOR in primary and metastatic HNSCC lesions

A. Detection of pS6 and vascular and lymphatic vessels in primary HNSCC lesions. Consecutive sections from a representative HNSCC lesion were stained with H&E, or immunostained for the phosphorylated form of S6, and the vascular (CD31) or lymphatic (LYVE1) endothelial markers, as indicated. Arrows point to the corresponding blood and lymphatic vessels, respectively. B. Microvessel quantification in primary HNSCC tumors immunoreacted with CD31 and LYVE 1 was performed as described in the methods section, using the IHC Microvessels Algorithm (Aperio, Vista, CA). Average and standard error of the mean (SEM) are presented for 5 representative HNSCC cases. Neither blood nor lymphatic vessels were observed in normal oral epithelium (not shown). C. Representative human metastatic lymph node from a patient with oral squamous cell carcinoma, stained for cytokeratins (CK, upper panel), pS6 (middle panel) and pAkt^{S473} (lower panel), showing the high levels of pS6 and pAkt^{S473} expression in the metastatic epithelial cells. The higher magnification show details of the malignant neoplastic cells; note how the areas showing pS6 and pAkt^{S473} expression superimpose with the epithelial cell marker cytokeratin. The graphic shows the percentage of pS6 and pAkt^{S473} positive tumors cells in invaded human lymph nodes with SCC tumors, as evaluated by immunohistochemistry. Average and standard error of the mean (SEM) are presented for 8 representative HNSCC cases with invaded lymph nodes.

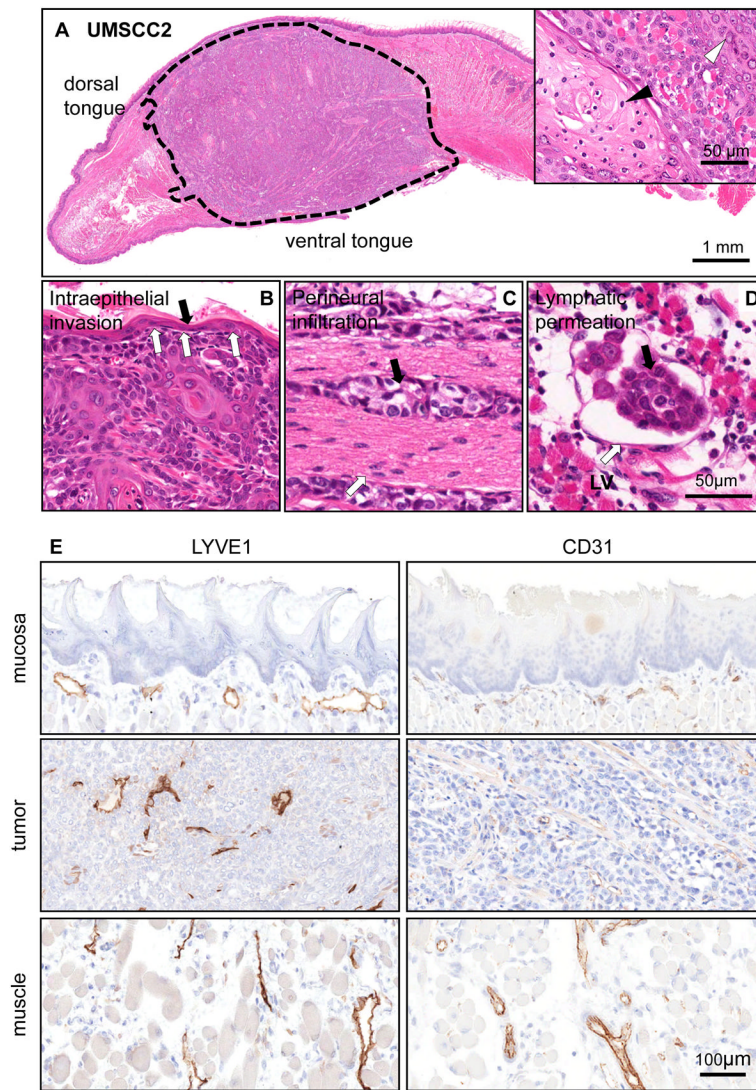


Figure 2. Local invasive growth and lymphangiogenesis of orthotopically implanted HNSCC cells into the tongue

A. H&E stained tissue section of a HNSCC orthotopic tumor (delimited with dotted line) growing into the anterior half of a tongue after 4 weeks post implantation. UMSCC2 is a well differentiated squamous cell carcinoma displaying keratinization (inset, black arrow head) and granular differentiation (inset, white arrow head). B. Intraepithelial invasion by HNSCC cells. The invasive area is indicated by the white arrows. The black arrow points to the remaining normal epithelium. C. Perineural infiltration. A group of HNSCC cells (black arrow) are seen growing surrounding a nerve structure (white arrow). This was a common finding in this orthotopic HNSCC model. D. Subepithelial lymphatic permeation by HNSCC cells. The carcinoma tends to grow inside the lymphatic vessels (LV); this finding was confirmed by immunohistochemistry (below). E. Immunohistochemistry identification of vascular (CD31) and lymphatic (LYVE 1) endothelial cells was performed and the results quantified in control mice and the HNSCC orthotopic tumors. No blood or lymphatic vessels are observed in normal epithelium. Normal mucosa included the epithelium and subepithelial area between the epithelium and the muscle; muscle refers to the normal skeletal muscle of the tongue, and tumor to the malignant epithelial area and its stroma.

includes the metastatic growth of UMSCC2 HNSCC cells in the area rounded by a dotted line. E. Using a dissection microscope, four to five cervical lymph nodes were isolated from each mice. These four pictures at a high magnification depict the histological features of a representative animal. Lymph nodes 1, and 2 show metastatic involvement, with the tumoral area (*) delimited by a dashed line; 3 and 4 show only reactive changes. F. Percentage of metastatic lymph nodes per animal in mice carrying orthotopic UMSCC2 HNSCC xenografts. Most mice developed cervical lymph nodes metastases within 5 weeks post-tumor cell implantation. G. A histological section of a non-invaded lymph node immunostained with anti-LYVE 1 antibody. A rich network of lymphatic vessels is evident in the cortical area of this node. The staining is mostly distributed in the cortical sinus and the cortex with less reactivity in the medulla. H. In a metastatic lymph node the growing HNSCC tumor (delimited by a dotted line) pushes the lymphatic ducts outward. Within the tumor parenchyma, a few ducts can be seen in the periphery (inset); the central area is necrotic and thus devoid of any structures.

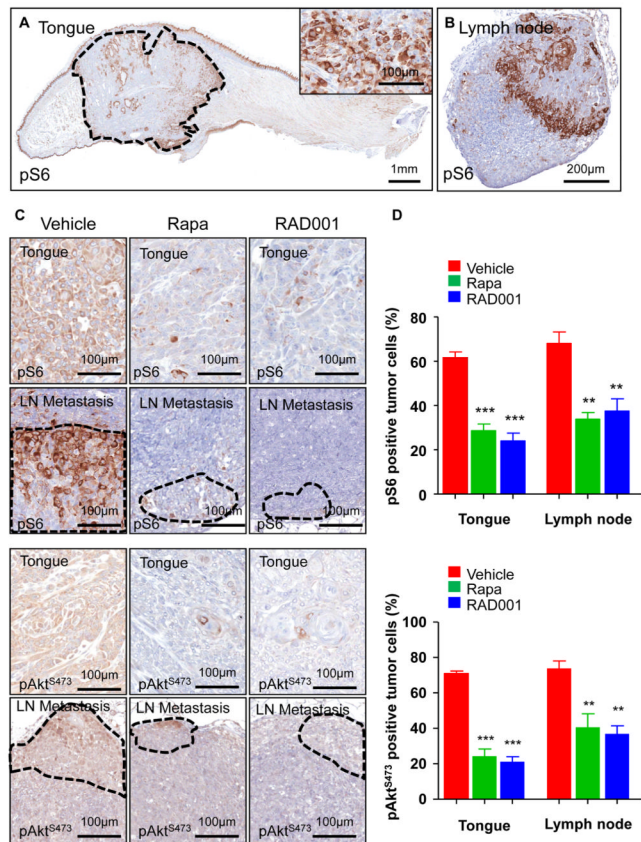


Figure 4. Inhibition of mTOR by rapamycin and RAD001 in HNSCC cells grown orthotopically into the tongue and in their spontaneous lymph node metastases

A. pS6 immunohistochemistry in UMSSC2 HNSCC orthotopic xenografts growing into a mouse tongue. The tumor area, circled by the dotted line, shows a high percentage of pS6-positive cells, as detailed in the inset. The suprabasal layers of the normal squamous epithelium of the tongue as well as other structures, such as the ducts of accessory salivary glands, are also positive. B. A representative metastatic cervical lymph node showing strong immunoreactivity for pS6 in the tumoral area. C. Detection of pS6 and pAkt^{S473} in HNSCC primary tumors and lymph node metastases in animals administered with vehicle control, rapamycin, and RAD001 for 48 h. There was a remarkable decrease in pS6 and pAkt^{S473} expression after rapamycin and RAD001 treatment. D. The graphic shows the percentage of pS6-positive (upper panel) and pAkt^{S473} (lower panel) tumor cells in primary HNSCC carcinomas (tongue) and their metastases (lymph node), as evaluated by immunohistochemistry. Rapamycin and RAD001 treatments induced a significant reduction in the number of positive cells in the treated tumors and metastases as compared with the control vehicle-treated group. *** p < 0.001, ** p < 0.01

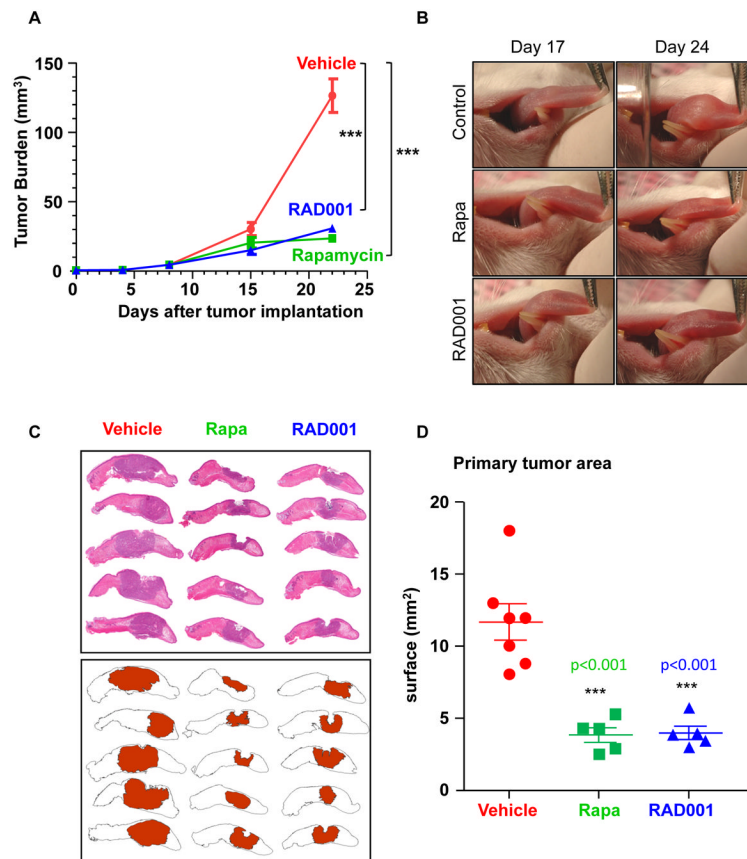


Figure 5. Inhibition of mTOR with rapamycin and RAD001 diminishes the growth of primary orthotopic HNSCC tumors

A. Tumor growth in UMSSC2 HNSCC orthotopic xenografts in control vs rapamycin- and RAD001-treated mice. Animals bearing HNSCC tumors into the tongue were randomized into the vehicle (n=37), rapamycin (n=25), and RAD001 (n=25) treated groups, and daily treatment regime initiated. All animals underwent weekly tongue evaluation and tumor growth quantified as described in the Methods section. B. Upper panels show the primary tumor of an early and late stage orthotopic HNSCC lesion treated with vehicle for the indicated days, while the lower panels show a representative mouse treated with rapamycin or RAD001. C. The pictures in the left panels show the individual tongues of representative mice in the vehicle-treated group vs. the rapamycin- and RAD001-treated animals (Rapa, middle, and RAD001, right groups, respectively). The tumor surface was mapped as described in Material and Methods and shown in red in the cartoon in the bottom panel. D. The compromised areas in each tongue were digitally quantified. The surface of the affected area per tongue for each vehicle control and rapamycin-treated mouse is indicated. Average and standard error for each group are indicated. *** p<0.001.

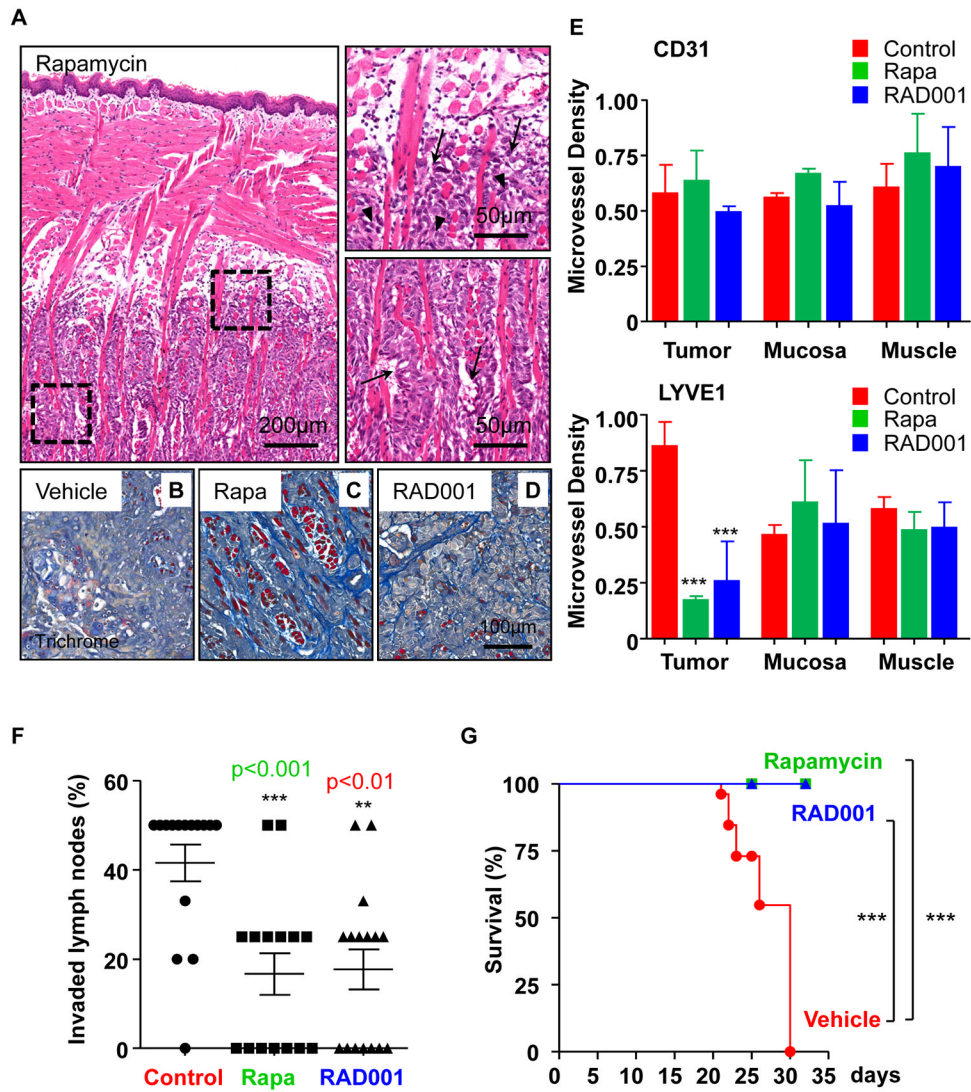


Figure 6. Inhibition of mTOR with rapamycin and RAD001 prevents the metastatic spread of primary HNSCC lesions to cervical lymph nodes, extending animal survival

A. Patterns of tumor regression in rapamycin- and RAD001-treated UMSSC2 HNSCC xenograft. After rapamycin treatment, the remnant tumor has become lobulated, with blocks of neoplastic cells divided by dense collagen strands. Similar results were observed in RAD001 treated animals (not shown). In the hematoxylin-eosin stained tissue (inset) the collagen is evident by an increase in eosinophilic material between the cells. The small pictures on the right are higher magnification of the areas depicted as dotted squares, showing two stages in rapamycin-induced regression within the same slide. On top, apoptotic images can be identified within the tumoral mass (arrow heads). In the bottom, intercellular edema and hemorrhages are evident. B–D. The increase in blue-stained collagen bands is evident in the rapamycin and RAD001 treated animal (C and D, respectively) as compared with the vehicle treated mouse (B). Masson trichrome staining. E. Microvessel quantification in primary HNSCC tumors immunoreacted with CD31 and LYVE 1. There were no significant differences in CD31 expression between vehicle controls and rapamycin or RAD001 treated tumors. Rapamycin and RAD001 administration induced a significant decrease of lymphatic vessels density specifically within the tumor

area, as judged by LYVE 1 staining (** $p < 0.001$). F. Percentage of metastatic lymph nodes in each animal in the vehicle- and rapamycin-treated groups. Rapamycin and RAD001 treatments induced a significant decrease the metastatic burden (** $p < 0.001$, * $p < 0.01$). G. Survival curve of mice carrying UMSSC2 HNSCC orthotopic xenografts treated with vehicle (n=26), rapamycin (n=20), and RAD001 (n=20). Treatment was started 10 days after HNSCC cell tongue implantation, when visible tumors were evident. As seen, all rapamycin and RAD001 treated animals were alive at the end of the study, while by contrast all animals in the vehicle-treated group succumbed to disease (** $p < 0.001$).